Pharm Res (2013) 30:2607–2624
DOI 10.1007/s11095-013-1087-3

RESEARCH PAPER

# Characterization of Damaged Skin by Impedance Spectroscopy: Chemical Damage by Dimethyl Sulfoxide

Erick A. White • Mark E. Orazem • Annette L. Bunge

Received: 13 February 2013 / Accepted: 19 May 2013 / Published online: 3 July 2013


## ABSTRACT

***Purpose*** To relate changes in the electrochemical impedance spectra to the progression and mechanism of skin damage arising from exposure to dimethyl sulfoxide (DMSO).

***Methods*** Electrochemical impedance spectra measured before and after human cadaver skin was treated with neat DMSO or phosphate buffered saline (control) for 1 h or less were compared with electrical circuit models representing two contrasting theories describing the progression of DMSO damage. Flux of a model lipophilic compound (p-chloronitrobenzene) was also measured.

***Results*** The impedance spectra collected before and after 1 h treatment with DMSO were consistent with a single circuit model; whereas, the spectra collected after DMSO exposure for 0.25 h were consistent with the model circuits observed before and after DMSO treatment for 1 h combined in series. DMSO treatments did not significantly change the flux of p-chloronitrobenzene compared to control.

***Conclusions*** Impedance measurements of human skin exposed to DMSO for less than about 0.5 h were consistent with the presence of two layers: one damaged irreversibly and one unchanged. The thickness of the damaged layer increased proportional to the square-root of treatment time until about 0.5 h, when DMSO affected the entire stratum corneum. Irreversible DMSO damage altered the lipophilic permeation pathway minimally.

**KEY WORDS** constant-phase element · DMSO · impedance spectroscopy · skin permeability · stratum corneum

## ABBREVIATIONS

| | |
|---|---|
| $a$ | constant in the interpolation formula for short and long time values of $x_d/L$ |
| $A$ | exposed skin area |
| $c$ | control experiment (as subscript) |
| $c_d$ | concentration of chemical at position $x_d$ within a membrane |
| $c_o$ | concentration of chemical in a membrane at the surface in contact with the solution containing the chemical |
| $C_s$ | capacitance of a capacitor in the R-C equivalent model circuit that exhibits the same characteristic frequency as the R-CPE equivalent circuit model |
| $C_{s,PL}$ | effective capacitance for an R-CPE equivalent model circuit with power-law decay of skin resistivity as proposed by Hirschorn *et al*. (36) |
| CPE | Constant-phase element |
| $f$ | frequency of the potential (voltage) perturbation in the measurement of impedance |
| $D$ | diffusion coefficient of the chemical in the membrane |

**Electronic supplementary material** The online version of this article (doi:10.1007/s11095-013-1087-3) contains supplementary material, which is available to authorized users.

E. A. White · A. L. Bunge (✉)
Chemical and Biological Engineering Department
Colorado School of Mines, 1500 Illinois Street, Golden,
Colorado 80401, USA
e-mail: abunge@mines.edu

M. E. Orazem
Department of Chemical Engineering, University of Florida
Gainesville, Florida 32611, USA

E. A. White
Currently at ITN Energy Systems, Littleton Colorado 80127, USA

| | |
|---|---|
| DMSO | Dimethyl sulfoxide |
| $f_c$ | characteristic frequency |
| $f_{c,d}$ | characteristic frequency observed for damaged SC |
| $f_{c,s}$ | characteristic frequency observed for undamaged SC |
| $f_{c,s\ before}$ | characteristic frequency observed for the SC before any treatment |
| $f_{c,t}$ | characteristic frequency for the low-resistance-pathways model calculated using $R_t$ for $R_s$ |
| $g$ | parameter in the definition for $C_{s,PL}$ |
| Hz | Hertz, unit of frequency (cycles per sec) |
| $j$ | $\sqrt{-1}$, unity in the complex plane |
| $L$ | thickness of the SC |
| $n$ | constant in the interpolation formula for short and long time values of in $x_d/L$ |
| nF | nanoFarad, units of capacitance |
| PBS | Phosphate buffered saline |
| PCNB | p-chloronitrobenzene |
| $pK_a$ | negative of the base-10 logarithm of the acid dissociation constant, $K_a$ |
| $Q$ | parameter characterizing the CPE in the equivalent circuit model |
| $Q_d$ | parameter characterizing the CPE in the equivalent circuit model of the damaged SC |
| $\widehat{Q}_d$ | length dependent parameter characterizing the CPE in the equivalent circuit model of the damaged SC |
| $Q_s$ | parameter characterizing the CPE in the equivalent circuit model of the undamaged SC |
| $\widehat{Q}_s$ | length dependent parameter characterizing the CPE in the equivalent circuit model of the undamaged SC |
| R-CPE | Model circuit consisting of a resistor (R) and CPE in parallel |
| $R_e$ | frequency-independent (Ohmic) resistance in series with the skin sample; consists of resistance of the electrolyte solution surrounding the skin sample, wires and possibly the dermis |
| $R_d$ | resistance of a resistor in the equivalent circuit model representing the damaged SC |
| $\widehat{R}_d$ | length dependent resistance of a resistor in the equivalent circuit model representing the damaged SC |
| $R_{lrp}$ | resistance of the low-resistance pathways arising from chemical damage |
| $R_s$ | resistance of a resistor in the equivalent circuit model representing the undamaged SC |
| $\widehat{R}_s$ | length dependent resistance of a resistor in the equivalent circuit model representing the undamaged SC |
| $R_t$ | total resistance of the parallel resistance through the SC and the low-resistance pathways arising from chemical damage |
| SC | Stratum corneum |
| $t$ | time |
| $t_{lag,d}$ | lag time for growth in the damaged layer |
| $x$ | position in a membrane measured from the surface in contact with the solution containing the chemical of interest |
| $x_d$ | thickness of the damaged layer within the SC |
| $Z$ | measured impedance; for an Ohmic material the ratio of the current and potential by Ohms law; $Z$ is a complex number |
| $Z_j$ | imaginary component of the impedance |
| $Z_r$ | real component of the impedance |
| $\alpha_s$ | parameter characterizing the CPE in the equivalent circuit model of the undamaged SC |
| $\alpha_d$ | parameter characterizing the CPE in the equivalent circuit model of the damaged SC |
| $\delta$ | position of the innermost interface of the dominant resistive layer; position within the SC with resistivity $\rho_\delta$ |
| $\varepsilon$ | dielectric constant of the SC (unitless) |
| $\varepsilon_d$ | dielectric constant of the damaged SC (unitless) |
| $\varepsilon_s$ | dielectric constant of the undamaged SC (unitless) |
| $\varepsilon_0$ | permittivity of a vacuum, $8.8542 \times 10^{-5}$ nF/cm |
| $\xi_{lrp}$ | parameter quantifying the relative contribution of the low-resistance pathways compared with the resistance of the undamaged SC |
| $\rho_\delta$ | resistivity of the innermost surface of the dominant resistive layer |
| $\Omega$ | Ohms, units of resistance |

## INTRODUCTION

In mammalian skin, the stratum corneum (SC) is often the primary barrier to chemical penetration as well as to the passage of electric current through the skin. Therefore, measurements of these in skin samples containing other skin layers (e.g., the viable epidermis and dermis) nearly always represent properties of the SC alone. The SC is itself heterogeneous, and measurements of both chemical

permeation and electrochemical impedance combine effects from the various structures within the SC.

Electrical properties of the SC, including sometimes structural information, can be deduced from electrochemical impedance spectroscopy. In this technique, the ratio of the change in potential to the change in current is determined over a range of frequencies (i.e., a spectrum) from the current or potential response to small amplitude modulation of an input current or potential (1). Additional background on the technique is provided in the previous paper (2), which showed that changes in the impedance spectra of skin after mechanical damage by needle puncture were consistent with the known change in structure. Electrical properties are linked with characteristics of some skin conditions and impedance can be used as a convenient noninvasive tool for assessing these conditions; e.g., hydration levels including changes with topical treatments (3–6), and the alteration and restoration of the skin following physical or electrical manipulations such as microneedles (7) or iontophoresis (8–12). Changes in impedance spectra also occur when skin is altered by exposure to chemicals, although systematic examination of this has been limited and the results understood poorly (13–17).

Many studies have shown that exposure to dimethyl sulfoxide (DMSO), a polar, aprotic solvent, alone or at concentrations larger than 60% by volume in water, causes irreversible changes to the skin barrier as measured by increases in chemical penetration (18–26) and decreases in low frequency impedance (17,24). Most of the changes in chemical penetration and impedance occur within the first 0.5 h (22,24), after which further change is small. Chemical penetration is enhanced even when DMSO is applied to both sides of the skin and the driving force for DMSO flux through skin is zero (19,20,25). Also, enhancement continued after DMSO exposure has ended (19,22). Therefore, added chemical flux is not due to active transport or direct carrying by DMSO (20).

There is evidence that DMSO damages the SC by elution of lipids (23,25,27) and delamination of the SC layer when DMSO was applied to one side, creating an osmotic gradient and cross-currents of water and DMSO (21,23,26). However, these mechanisms likely operate too slowly to explain the magnitude of the changes in impedance and permeation that occur in less than 0.5 h. It has been shown that both lipids and proteins in the SC are progressively altered by skin exposure to DMSO. Specifically, lipids are changed from the predominant all trans gel phase to trans-gauche liquid crystalline phase (28,31). DMSO may also interact with the lipid polar head groups, perhaps replacing water to cause expansion of the hydrophilic region between the lipid polar head groups (28,29). Proteins in the SC, predominantly keratin, change in the presence of DMSO from $\alpha$-helical to a $\beta$-sheet conformation to an extent that depends on the concentration of free water, suggesting that DMSO displaces bound protein water (28,30). The lipid changes only occur at the DMSO concentrations that also produce increased chemical penetration (or reduced impedance), while keratin changes occur at concentrations as small as 20%, suggesting that lipid interactions may be critical to penetration enhancement.(28,29). In addition to these mechanisms, large concentrations of DMSO within the SC may increase the ability of chemicals to partition into the SC (29). The time required for DMSO to penetrate through and complete the alteration of lipids and proteins in the SC layer is less than 1 h (28) and perhaps as short as 15–20 min (30,31).

The present work was the second of two studies that had the overall goal of using impedance spectroscopy to characterize and understand changes in skin barrier function following irreversible damage. The objective of the first study was to examine the effect of a mechanical insult, namely needle puncture (2). The primary objective of this study was to quantify the effect of 100% DMSO for treatment times of 1 h or less on the impedance spectra. A secondary objective was to acquire preliminary information on the effect of irreversible DMSO damage to the permeation barrier for lipophilic compounds. Therefore, the steady-state flux of a model lipophilic chemical, p-chloronitrobenzene (PCNB) was determined coincidentally with the impedance measurements.

As observed in previous studies, impedance decreased with increasing exposure time to a minimum value that was reached within 1 h. Two contrasting theories on the progression of DMSO damage are proposed. In the first, DMSO damages an increasing fraction of the SC thickness over time without changing the intrinsic electrical properties of the undamaged SC fraction from their before treatment values. According to this two-layer scheme, the observed decrease in the magnitude of the impedance is due to a decrease in the thickness of undamaged SC. In the second theory, DMSO acts by increasing the contributions of low-resistance pathways through the SC by any of three indistinguishable mechanisms: opening new pathways (i.e., increasing the number of pathways), increasing the area of these pathways, or decreasing the effective length of these pathways. Assuming further that DMSO does not otherwise change the SC, then the mechanism of impedance decrease with DMSO is similar to administering multiple needle punctures to the SC over time. Circuit models consistent with the nature of skin damage by these two different theories are proposed and compared with the experimental observations.

## THEORY

Skin impedance is related to the structure and composition of the SC. In this study the skin barrier is altered by chemical damage arising from exposure on both sides of the skin to DMSO. Circuit models are proposed to describe the resulting skin impedance.

## Skin Impedance Models

It is common for skin impedance spectra to be consistent with the frequency behavior of the R-CPE circuit model depicted in Fig. 1a. This model consists of a parallel resistor ($R_s$) and constant-phase element (CPE), which represent the impedance response of the SC, in series with a frequency-independent Ohmic resistance ($R_e$), which characterizes the resistance from the electrolyte, wires and possibly the viable epidermis and dermis. The impedance ($\mathcal{Z}$) of the R-CPE circuit model varies with frequency ($f$) as

$$\mathcal{Z} = R_e + \frac{R_s}{1 + R_s Q_s (j2\pi f)^{\alpha_s}} \tag{1}$$

where $j$ is the complex number $\sqrt{-1}$, and the parameters $Q_s$ and $\alpha_s$ define the CPE behavior (1). Expressions for the real and imaginary components of Eq. (1) are provided in the Appendix. The impedance for an R-CPE circuit is characterized by a single characteristic frequency ($f_{c,s}$), defined as the frequency at which the absolute value of the imaginary part of the impedance is maximized; it may be expressed in terms of the CPE parameters $Q_s$ and $\alpha_s$ (2) as

$$f_{c,s} = \frac{1}{2\pi \left(R_s Q_s\right)^{1/\alpha_s}} \tag{2}$$

As shown below, impedance spectra for skin treated with DMSO for longer periods of time are also consistent with the R-CPE circuit model. However, the characteristic frequency after DMSO treatment of the skin ($f_{c,d}$) is significantly larger than the characteristic frequency before treatment ($f_{c,s}$), which is consistent with a damaged SC showing reduced resistance ($R_d$) and altered CPE parameters ($\alpha_d$ and $Q_d$) in Eq. (2).

In the fraction-damaged model, it is hypothesized that SC treated with DMSO for shorter periods of time will consist of two layers as illustrated in Fig. 2: an undamaged layer (identified with the subscript s) and a damaged layer (identified with the subscript d). Because DMSO was applied to both sides of the skin, the schematic in Fig. 2 depicts the total thickness of the DMSO damaged SC ($x_d$) as two damaged layers (i.e. the non-shaded regions) of equal thickness ($x_d/2$), although the assumption of an equal division is unnecessary for the following analysis. The presence of two layers in the SC, one damaged and one undamaged, can be represented by the fraction-damaged circuit model depicted in Fig. 1b with $R_e$ in series with two circuits each consisting of a parallel resistor and CPE. The impedance of this circuit model may be expressed as

$$\mathcal{Z} = R_e + \frac{\widehat{R}_s}{1 + \widehat{R}_s \widehat{Q}_s (j2\pi f)^{\alpha_s}} + \frac{\widehat{R}_d}{1 + \widehat{R}_d \widehat{Q}_d (j2\pi f)^{\alpha_d}} \tag{3}$$

where the R-CPE parameters for the undamaged and damaged skin layers are identified by the subscript s and d, respectively. The hats on $\widehat{R}$ and $\widehat{Q}$ for each layer designate that the values of these parameters are dependent on the thickness of the damaged layer ($x_d$) relative to the total SC thickness ($L$).

Under the assumption that longer exposure to DMSO causes the damaged layer thickness to increase without changing the average electrical properties (e.g., resistivity and dielectric constant) of the undamaged and damaged layers, the impedance may be expressed in terms of the relative thickness of the damaged layer ($x_d/L$) as

$$\mathcal{Z} = R_e + \left[\frac{R_s}{1 + R_s Q_s (j2\pi f)^{\alpha_s}}\right]\left(1 - \frac{x_d}{L}\right) + \left[\frac{R_d}{1 + R_d Q_d (j2\pi f)^{\alpha_d}}\right]\frac{x_d}{L} \tag{4}$$

Length-independent values of $R$ and $Q$ for the undamaged and damaged layers are derived by comparing Eqs. (3) and (4) to yield

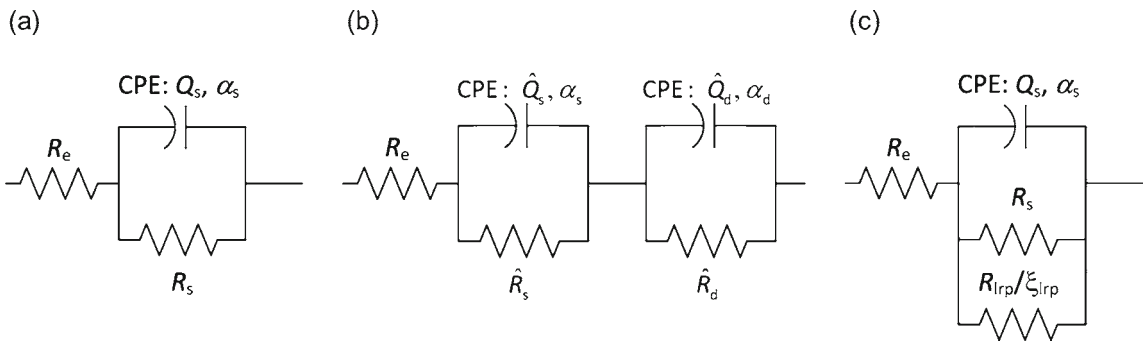


**Fig. 1** Equivalent circuit models used to describe undamaged SC and SC that is damaged chemically by DMSO: (**a**) one R-CPE circuit describing undamaged SC or uniformly damaged SC, (**b**) fraction-damaged model of two R-CPE circuits in series describing creation of a damaged SC layer, and **c** low-resistance-pathways model of the one R-CPE circuit with an additional parallel resistance describing damage that creates a low-resistance pathway.

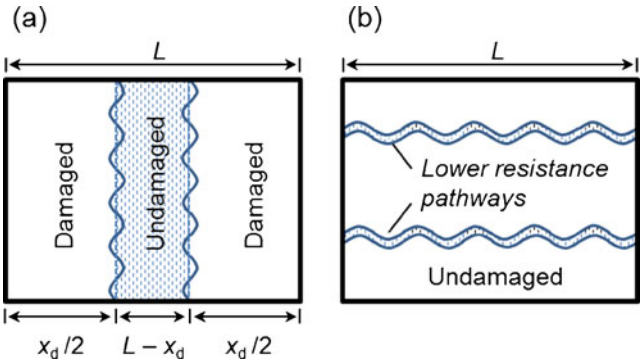


**Fig. 2** Schematic representation of two contrasting theories for DMSO damage of the stratum corneum: (**a**) fraction-damaged model; and (**b**) low-resistance-pathways model.

$$R_s = \frac{\widehat{R}_s}{\left(1 - x_d/L\right)} \tag{5}$$

$$Q_s = \widehat{Q}_s\left(1 - x_d/L\right) \tag{6}$$

$$R_d = \frac{\widehat{R}_d}{x_d/L} \tag{7}$$

and

$$Q_d = \widehat{Q}_d\left(x_d/L\right) \tag{8}$$

The characteristic frequencies of the R-CPE circuits representing the undamaged and damaged layers ($f_{c,s}$ and $f_{c,d}$, respectively) can be calculated using either the length-dependent values ($\widehat{R}$ and $\widehat{Q}$) or the length-independent values ($R$ and $Q$) for $R_s$ and $Q_s$ in Eq. (2). The frequency dependence in the impedance response described by Eqs. (3) and (4) is characterized by two convoluted time constants that are equal to $1/f_{c,s}$ and $1/f_{c,d}$.

An assumption in the development of Eqs. (3) and (4) is that the interface between the damaged and undamaged SC layers is a distinct plane parallel to the skin surface and across the area of the DMSO treated skin. However, it is likely that DMSO does not affect the SC uniformly, resulting in an interface of finite thickness between the damaged and undamaged parts of the skin. This situation is represented schematically in Fig. 2 by the solid, wavy lines. This should not impact the theoretical description presented here provided the thickness of the interface is small relative to the SC thickness.

In the alternative to the fraction-damaged model, decreasing impedance with increasing periods of DMSO exposure is explained by increasing contributions of low-resistance pathways. This scenario can be represented by the low-resistance-pathways model depicted in Fig. 1c, for which the impedance may be expressed as

$$\mathcal{Z} = R_e + \frac{R_t}{1 + R_t Q_s (j2\pi f)^{\alpha_s}} \tag{9}$$

In this model $Q_s$ and $\alpha_s$ are assumed to be unchanged by DMSO treatment, and $R_t$, defined as

$$R_t = \left[\frac{1}{R_s} + \frac{\xi_{lrp}}{R_{lrp}}\right]^{-1} \tag{10}$$

is the total resistance of the new low-resistance pathways created by the DMSO treatment ($R_{lrp}/\xi_{lrp}$) operating in parallel with the undamaged SC ($R_s$). The parameter $\xi_{lrp}$, which quantifies the relative contribution of the low-resistance pathways compared with the resistance of the damaged SC resistance, increases with DMSO exposure time. For convenience, $R_{lrp}$ is defined such that $R_t$ is equal to the damaged SC resistance $R_d$ when $\xi_{lrp}$ is 1. Thus,

$$R_{lrp} = \left[\frac{1}{R_s} - \frac{1}{R_d}\right]^{-1} \tag{11}$$

Although the notation has been altered, this low-resistance-pathways model is identical in form to the pinhole model presented in the companion paper (2), which described skin damaged by one or more needle punctures. Like undamaged skin and skin that has been treated with DMSO for a long enough time, the low-resistance-pathways model exhibits a single characteristic frequency, $f_{c,t}$, which is calculated by substituting $R_t$ for $R_s$ in Eq. (2).

## Impedance Model Behavior

Graphs of the area ($A$) normalized real and imaginary components of the impedance (i.e., $\mathcal{Z}_r A$ and $-\mathcal{Z}_j A$) as well as $d \log(-\mathcal{Z}_j A)/d \log(f)$ plotted as a function of frequency each reveal different features of the impedance response for a given circuit model. In Fig. 3, the impedance behavior predicted by the fraction-damaged and low-resistance-pathways models of DMSO damage are compared and contrasted.

The impedance behavior predicted by the fraction-damaged model described by Eq. (4) is illustrated in the left-hand column of Fig. 3 for $R_e = 0.15$ kΩ and input parameter values that were reasonable for human SC (based on experimental results presented subsequently): the undamaged SC layer is represented by regression results for sample B before treatment with DMSO for 0.25 h ($R_s A = 167.0$ kΩ cm$^2$, $\alpha_s = 0.862$, $Q_s/A = 41.4$ nF $s^{\alpha_s - 1}$/cm$^2$ and $f_{c,s} = 51$ Hz) and the damaged layer is represented by the mean of the regression parameters for the three samples treated with DMSO for 1 h ($R_d A = 1.36$ kΩ cm$^2$, $\alpha_d = 0.81$, $Q_d/A = 152$ nF $s^{\alpha_s - 1}$/cm$^2$ and $f_{c,d} = 5{,}640$ Hz). The impedance response is shown for the

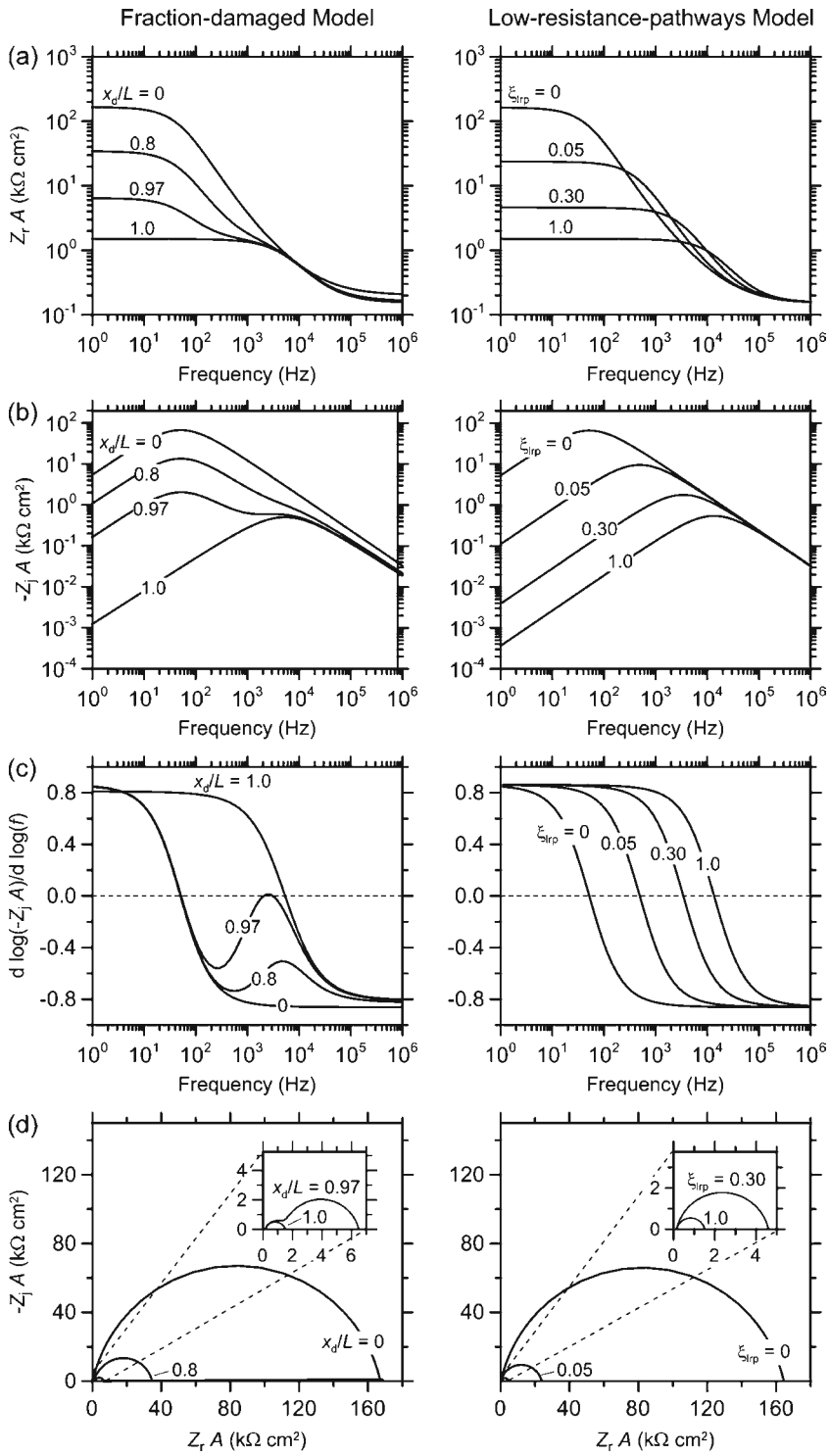


**Fig. 3** Comparison of impedance spectra calculated using the fraction-damaged model for varying $x_d/L$ and the low-resistance-pathways model for varying $\xi_{lrp}$: (**a**) area normalized real component *versus* frequency, (**b**) area normalized imaginary component *versus* frequency, (**c**) local slope of the log-log plot of the area normalized imaginary part of the impedance *versus* frequency, and (**d**) impedance plane (Nyquist) plot showing the area normalized imaginary and real parts of the impedance. The model parameters used in the calculation are typical of those observed in this study: $R_e A = 0.150$ kΩ cm$^2$, $R_s A = 167.0$ kΩ cm$^2$, $R_d A = 1.36$ kΩ cm$^2$, $Q_s/A = 41.4$ nF $s^{\alpha_s - 1}$/cm$^2$, $Q_d/A = 152$ nF $s^{\alpha_s - 1}$/cm$^2$, $\alpha_s = 0.862$, $\alpha_d = 0.81$, $f_{c,s} = 51$ Hz, $f_{c,d} = 5{,}640$ and $R_{lrp} A = 1.37$ kΩ cm$^2$.

relative thickness of the damaged layer ($x_d/L$) varying from zero (i.e., no damage) to one (i.e., fully damaged).

When $x_d/L = 0$ or $x_d/L = 1$, the frequency dependence is consistent with the R-CPE model described by Eq. (1). For $x_d/L$ values between 0 and 1, the characteristic frequencies corresponding to two R-CPE circuits, representing the undamaged and damaged SC layers, both contribute to the total impedance. Thus, although the magnitude of the impedance changes with $x_d/L$, the characteristic frequency of each layer remains unchanged. In skin, this is consistent with the relative thicknesses of the undamaged and damaged SC layers decreasing and increasing, respectively,

while the R-CPE parameters ($R$, $Q$ and $\alpha$) for each layer remain constant.

Impedance features can be identified in plots of d log($-\mathcal{Z}_j A$)/d log($f$) *versus* frequency (see Fig. 3c) that are not readily visible in other graphical representations. Consistent with a circuit characterized by one characteristic frequency, plots of d log($-\mathcal{Z}_j A$)/d log($f$) decrease monotonically with frequency from the low frequency limit (either $\alpha_s$ or $\alpha_d$) to the high frequency limit (either $-\alpha_s$ or $-\alpha_d$) crossing zero at the characteristic frequency (either $f_{c,s}$ or $f_{c,d}$) when the SC is either completely undamaged or completely damaged (i.e., $x_d/L=0$ or $x_d/L=1$). However, when the SC is partially damaged (i.e., $0<x_d/L<1$), contributions from both layers are apparent if $f_{c,s}$ and $f_{c,d}$ are sufficiently different. In this situation, plots of d log($-\mathcal{Z}_j A$)/d log($f$) decrease monotonically with frequency from the low-frequency limit (equal to the smaller of $\alpha_s$ or $\alpha_d$) to cross zero at a frequency close to the characteristic frequency of undamaged skin ($f_{c,s}$). As the frequency increases towards the characteristic frequency of damaged skin ($f_{c,d}$), inflections or a local minimum and maximum are observed, followed by a monotonic decrease to the negative of the low frequency limit. Compared with the d log($-\mathcal{Z}_j A$)/d log($f$) *versus* frequency plots, it is much more difficult to identify the simultaneous presence of damaged and undamaged SC layers in plots of $-\mathcal{Z}_j A$ or $\mathcal{Z}_r A$ *versus* frequency, which introduces subtle inflection points near the characteristic frequency of damaged skin that are most apparent, although still difficult to see, when $x_d/L=0.97$. Likewise, it is nearly impossible to discern that there are contributions from two separate R-CPE circuits from an impedance plane (Nyquist) plot, which compares $-\mathcal{Z}_j A$ against $\mathcal{Z}_r A$ (Fig. 3d).

The impedance behavior of the fraction-damaged model can be compared with the model assuming DMSO has created new low-resistance pathways through the otherwise undamaged SC, which is shown in the right-hand column of Fig. 3. In these calculations, the undamaged SC properties were assumed to be the same as in the fraction-damaged model calculations and $R_{lrp} A$ was 1.37 kΩ cm$^2$, which is consistent with $R_t A=R_d A$ when $\xi_{lrp}=1$. The impedance response is presented for the relative contributions of the low-resistance pathways ($\xi_{lrp}$) increasing from 0 to 1.

The predicted impedance responses of the fraction-damaged and low-resistance-pathways models are similar in a few respects. At low frequency, the real and imaginary parts of the impedance, indicated by $\mathcal{Z}_r A$ and $-\mathcal{Z}_j A$, respectively, decrease with increasing damage (i.e., with larger values of $x_d/L$ and $\xi_{lrp}$). At high frequency, values of $\mathcal{Z}_r A$ approach $R_e A$ independent of the amount of DMSO damage. Here the similarities end. At high frequency, $\mathcal{Z}_j A$ is unaffected by the extent of damage in the low-resistance-pathways model (i.e., the high frequency limit for $\mathcal{Z}_j A$ is independent of $\xi_{lrp}$), but decreases with increasing thickness of the DMSO damaged layer. Plots of d log($-\mathcal{Z}_j A$)/d log($f$) *versus* frequency for skin damaged due to low-resistance pathways decrease monotonically with frequency from $\alpha_s$ to $-\alpha_s$, and never exhibit the inflections or local maximum or minimum that are predicted by the fraction-damage model because the impedance spectra from the undamaged and damaged layers of the SC are convoluted.

If DMSO damage occurs through low-resistance pathways, then the characteristic frequency, which is the frequency at which the $-\mathcal{Z}_j A$ curves are maximized or where d log($-\mathcal{Z}_j A$)/d log($f$) equals zero, increases as the amount of damage increases. In contrast, for the fraction-damaged model, the frequency at which the $-\mathcal{Z}_j A$ curves are maximized or where d log($-\mathcal{Z}_j A$)/d log($f$) equals zero does not change as $x_d/L$ increases until $x_d/L=1$. Differences in the Nyquist plots for the two damage models are only apparent when the damage is almost complete (i.e., $x_d/L=0.97$), making this graphical analysis unsuitable for identifying the damage mechanism. However, the several clear differences in the other graphical representations of the impedance responses from the fraction-damaged and low-resistance-pathways model provide the opportunity to assess experimentally the mechanistic origins of SC damage from DMSO exposure.

## MATERIALS AND METHODS

Impedance spectra and chemical flux were measured before and after skin was chemically damaged using DMSO following similar procedures to those described in the companion study of pinhole damage (2). Experimental details for methods that were used in both studies are provided in the paper describing the pinhole study (2). The experimental descriptions specific to this study are described below.

### Chemicals and Materials

Permeation of p-chloronitrobenzene (PCNB, CAS 100-00-5, molecular weight = 157.6 Da, logarithm of the octanol-water partition coefficient = 2.4) or 4-cyanophenol (CAS 767-00-0, molecular weight = 119.1 Da, logarithm of the octanol-water partition coefficient = 1.6), both purchased from Sigma, was measured before and after split-thickness human cadaver skin (from either the back or abdomen of a 78-year old Caucasian male identified as subject AS) was treated with DMSO (99.9%, CAS 67-68-5) from Fisher Scientific. Skin (300–400 μm thick) collected within 24 h and frozen immediately was purchased from the National Disease Research Interchange (NDRI, Philadelphia, PA) and stored at –60°C or below until used.

### Skin Impedance Measurements

Impedance was measured in the four-electrode configuration using a Gamry potentiostat (model PCI4/300, Warminster, PA). A 10 mV root-mean-squared, sinusoidal alternating current perturbation signal with a mean applied potential of zero (i.e., no direct current bias) was applied at 10 frequencies per logarithmic decade over the frequency range of 1 Hz to 100 kHz.

### DMSO Experiments

The DMSO experiments consisted of simultaneous measurements of impedance and PCNB flux through skin in four diffusion cells before and after four different treatments: 0.25 and 1 h treatments with 100% DMSO or with PBS, which acted as the control. The entire experiment, which followed the steps shown in Fig. 4, was repeated three times. For each treatment, skin was mounted into a frame, which was then clamped into a side-by-side diffusion cell from PermeGear, (Hellertown, PA) that had been modified to hold 2 electrodes in both the donor and receptor chambers as described previously (2). The frame was designed such that the skin sample can be removed from and returned to the diffusion cell easily after performing a treatment outside the diffusion cell. Experiments were conducted 32°C. Additional experimental details are provided in reference (2).

Both chambers of the diffusion cell were filled with PBS for an eight to twelve hour equilibration period in which impedance spectra were measured hourly. After equilibration, both chambers were emptied and the receptor and donor chambers were rinsed and filled with 13 mL of PBS and PCNB-saturated PBS, respectively. To ensure saturation of the donor solution throughout the experiment, excess crystals of PCNB were added to the donor chamber solution. One-milliliter samples, collected periodically from the receptor chamber, were replaced with an equal volume of chemical-free PBS. A total of nine samples were collected over 8 h. The first sample was collected between 0 and 0.5 h after the introduction of the donor solution. The eight subsequent samples were collected approximately hourly relative to the time that the saturated donor solution was introduced to the donor chamber. Impedance scans were also collected approximately hourly during the permeation study. Next, the receptor and donor chambers were emptied and filled with either DMSO or with PBS (for the control experiments). After treatment for either 0.25 or 1 h, the frame holding each skin sample, including the PBS controls, was removed from the diffusion cell assembly. The four frames were soaked together in approximately 1 L of fresh deionized water three times for 0.25 h and then for 1 h in about 1 L of PBS. The diffusion cells were rinsed thoroughly and then reassembled and filled with PBS solution for another 8-h equilibration period with hourly impedance scans. After this, the PCNB flux measurements were repeated. Impedance results reported for before and after DMSO treatment were derived from the last spectrum collected during the equilibration periods.

In a separate pilot study of treatment time conducted before the study described above, four skin samples were each treated with DMSO for one of four different times: 0.25, 0.5, 0.75 and 1 h. All four experiments ($n=1$ at each treatment time) were done at the same time following the same procedure described above except that 4-cyanophenol was used in the permeation study rather than PCNB.

### Analytical Methods and Data Analysis

The details of the impedance and chemical analysis by high performance liquid chromatography have been described

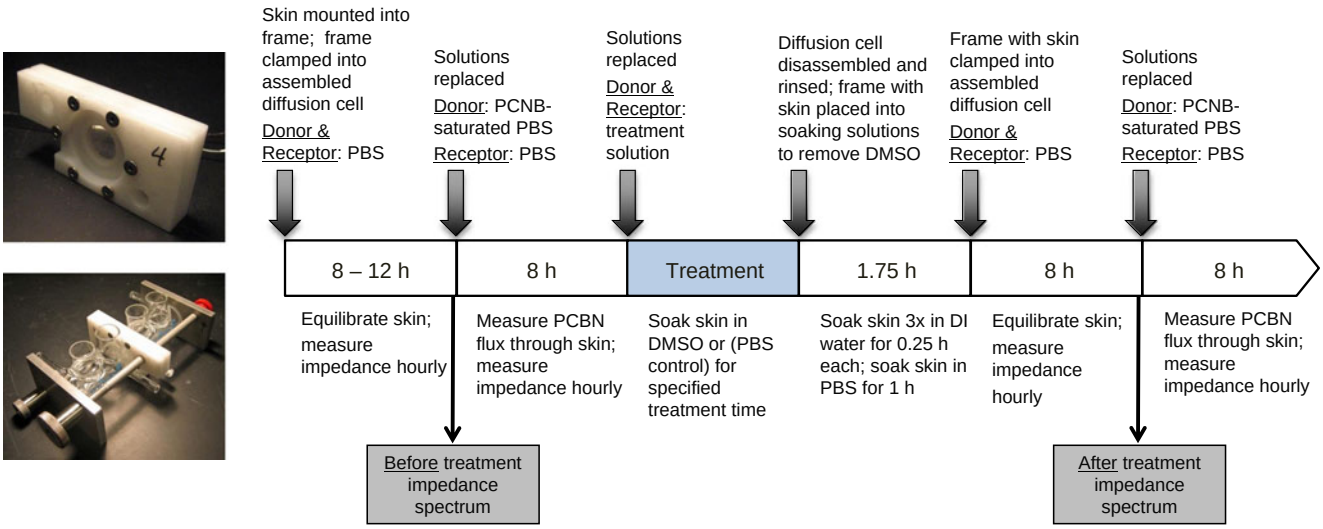


**Fig. 4** Photos of the frame alone and clamped into diffusion cell and a schematic diagram of the experimental protocol.

previously (2). To determine concentrations of PCNB, the diode array detector was set to 274 nm and the flow rate of the mobile phase of acetonitrile and water (70:30 v:v) was 1.5 mL/min, which gave a retention time of about 3.7 min. In the 4-cyanophenol analysis, the detector was set to 254 nm and the retention time was about 2.3 min using the same mobile phase as PCNB flowing at 1 mL/min. Determinations of the steady-state flux and the best-fit values of the parameters in the various equivalent circuit models were determined following the same procedures as in the study of pinhole damaged skin (2). Unless noted differently, results are reported as the mean value ± one standard deviation and the student t-test with the requirement of $p<0.05$ was used to assess the statistical significance of mean values for either paired measurements (e.g., before and after values) or two different groups of measurements.

## RESULTS AND DISCUSSION

The influence of DMSO exposure on skin properties was assessed by impedance spectroscopy. The appearance of a second characteristic frequency in the impedance measured after a short exposure to DMSO was used to differentiate between the two hypothesized damage models. An analysis of dielectric constants extracted from the impedance response was used to support the interpretation based on impedance. The influence of DMSO exposure on the flux of PCNB was also explored.

### Skin Impedance

In Fig. 5, graphs of the area-normalized real ($\mathcal{Z}_r A$) and imaginary ($-\mathcal{Z}_j A$) components of the impedance, as well as the slope of the $\log(-\mathcal{Z}_j A)$ *versus* $\log(f)$, are plotted as functions of frequency for the six skin samples measured before and after DMSO treatment for either 0.25 h (samples A, B and C) or 1 h (samples D, E and F). Spectra collected before treatment are shown in the left column; spectra measured after DMSO treatment for 0.25 h and 1 h are presented in the middle and right columns, respectively. On average, $\mathcal{Z}_r A$ at low frequency decreased by factors of ~4 and ~100 after 0.25 and 1 h DMSO treatment, respectively, while DMSO treatment at both times had no effect on the $\mathcal{Z}_r A$ at the highest frequencies. Consistent with the theoretical impedance curves for the fraction-damaged model shown in Fig. 3, the impedance spectra of skin before DMSO treatment and after DMSO treatment for 1 h each exhibit one characteristic frequency as predicted by the one R-CPE circuit model (corresponding to $x_d/L$ equal to 0 and 1, respectively); whereas, the impedance spectra of the 0.25 h DMSO treated samples behaved as predicted by the fraction-damaged model. This is most clearly evident in the plot of $d\log(-\mathcal{Z}_j A)/d\log(f)$, which, as predicted by the fraction-damaged model (Fig. 3c), exhibits a minimum (at about 1,000 Hz) and a maximum (at ~10,000 Hz). The impedance response is clearly inconsistent with the low-resistance-pathways model.

There are a few other observations worth noting. The impedance spectra before DMSO treatment show considerable sample-to-sample variation in the magnitude of the low-frequency impedance and the characteristic frequency, which corresponds to the frequency where $d\log(-\mathcal{Z}_j A)/d\log(f)$ crosses zero. Variability is significantly reduced in skin that was treated with DMSO for 1 h. Accordingly, the characteristic frequencies for these three samples are in close agreement with the average $f_{c,d}$, indicated by the vertical line through the 1-h DSMO treatment data in Fig. 5. Even the data scatter in the low frequency values of $d\log(-\mathcal{Z}_j A)/d\log(f)$ has a similar appearance, which almost certainly arises because the magnitude of $-\mathcal{Z}_j A$ is small enough to be affected by instrument noise.

The impedance results for four skin samples after DMSO treatment for 0.25, 0.5, 0.75 and 1 h (samples G, H, I and J, respectively) are shown in Fig. 6. Because this experimental series was conducted as a pilot test to choose treatment times for the study described above, it was not replicated. It is included here because the results, which are consistent with the other measurements, clearly illustrate the progression of the DMSO damage over time. The $\mathcal{Z}_r A$, $-\mathcal{Z}_j A$ and $d\log(-\mathcal{Z}_j A)/d\log(f)$ spectra for the two skin samples treated with DMSO for 0.25 and 1 h are consistent with the impedance spectra of the samples treated for the same times shown in Fig. 5. Like the results shown in Fig. 5, the magnitude and frequency dependence of the impedance spectra presented in Fig. 6 are consistent with the theoretical curves of the fraction-damaged model in Fig. 3.

After DMSO treatment for 0.5 h, the two convoluted spectra appear as a broad peak in the $(-\mathcal{Z}_j A)$ spectrum. Like the theoretical calculations presented in Fig. 3, the presence of two R-CPE spectra with two characteristic frequencies is more apparent in the $d\log(-\mathcal{Z}_j A)/d\log(f)$ plot in Fig. 6c for treatment times of 0.25 and 0.5 h, where the contribution of the second characteristic frequency causes a change of slope in the $d\log(-\mathcal{Z}_j A)/d\log(f)$ curve between 100 and 200 Hz. After DMSO treatment for 0.75 h, the impedance response is consistent with a nearly completely damaged SC layer with a dominant characteristic frequency at high frequency similar to skin treated with DMSO for 1 h. There is a small contribution from the undamaged layer at lower frequencies that is evident by the deviation of the $-\mathcal{Z}_j A$ spectrum from the spectrum after 1 h DMSO treatment.

The skin impedance data shown in Fig. 5 were regressed to the one or two R-CPE equivalent circuit models described above to give the results for skin resistance and the CPE parameters that are summarized in Fig. 7 and reported

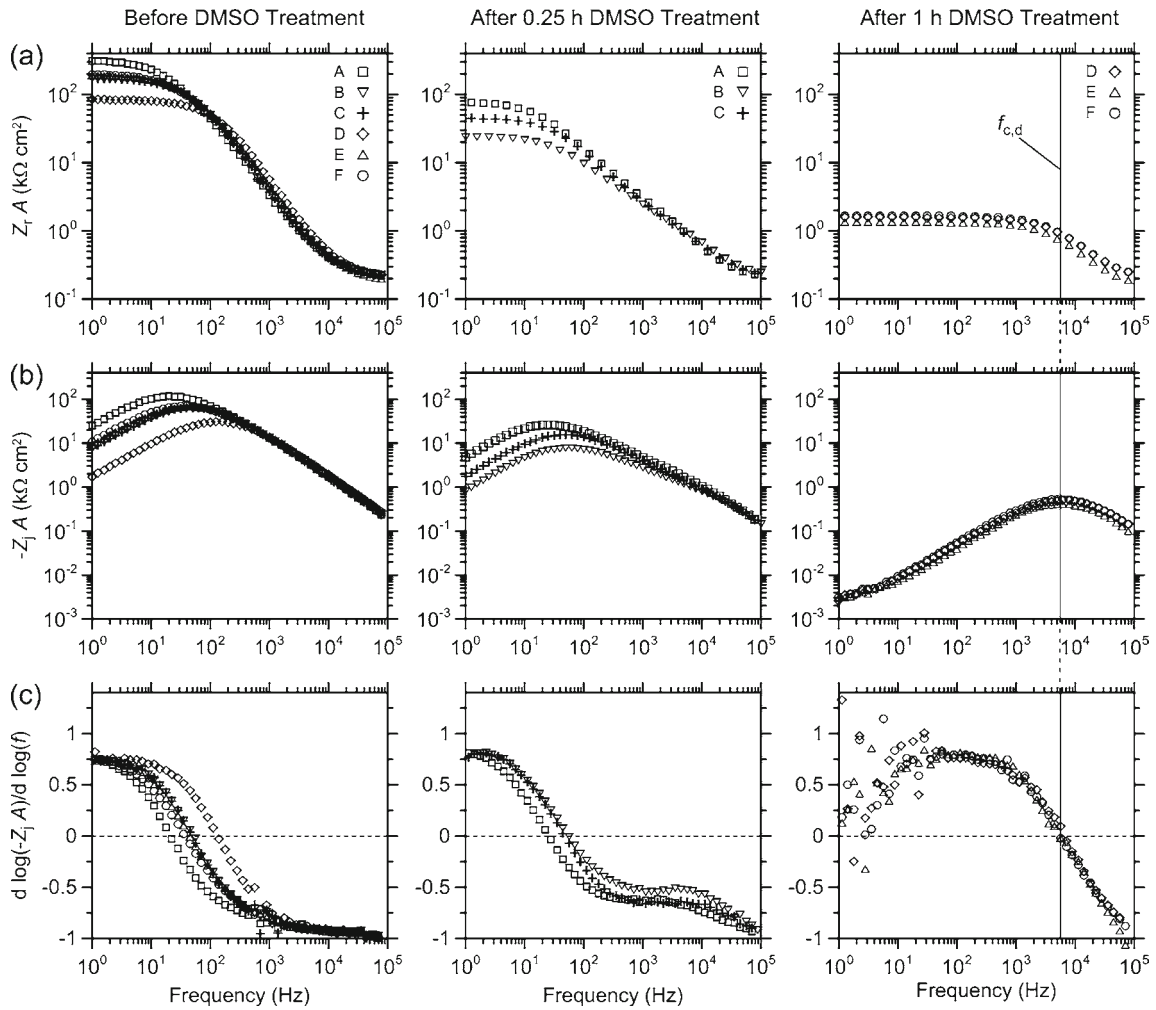


**Fig. 5** Impedance spectra as a function of the frequency before and after skin is treated with DMSO for 0.25 and 1 h: (**a**) area normalized real part of the impedance, (**b**) area normalized imaginary part of the impedance, and (**c**) local slope of the log-log plot of the area normalized imaginary part of the impedance with frequency.

in more detail, including the standard error for the regressed parameters, in the Supplementary Material (Tables S.I–S.III). Except for $\widehat{Q}_d/A$ (see Table S.III), all values of the regressed parameters were determined with a high degree of confidence as indicated by the small errors. The inability to resolve $\widehat{Q}_d/A$ with more certainty is likely due to the convolution of the small-impedance damaged layer with the large-impedance undamaged layer.

Although not shown in Fig. 7, as expected, $R_e A$ was unaffected by treatment and determined to be 0.142 ± 0.023 kΩ cm$^2$ for all 12 samples before and after treatment, which was nearly always less than 1% of the total skin resistance except after skin was treated with DMSO for 1 h (see Tables S.I and S.II in the Supplementary Material). After treatment with PBS, $Q_s/A$ and $\alpha_s$ did not change, but $R_s A$ decreased by a small amount that was independent of the treatment time (Fig. 7a). On average, $R_s A$ after treatment was 86% of the value in the same piece of skin before treatment. After treatment with DMSO for 1 h, $\alpha$ decreased slightly, $Q/A$ increased by about 4 fold, and $R_d A$ dropped nearly two orders of magnitude to 1.4 kΩ cm$^2$, which was independent of the before treatment value (Fig. 7). This value for $R_d A$ is similar to 1.9 kΩ cm$^2$ reported by Allenby *et al.* (25) for skin that was treated with 100% DMSO for 0.5 h, which was long enough to observe what they called the "maximum effect" (note that $A = 0.8$ cm$^2$ in their experiments is reported in a companion paper (24)).

When $Q/A$ was determined by regression of the spectra measured after DMSO treatment for 0.25 h to a single R-CPE model (identified as "After combined" in Fig. 7b), the results are anomalously high (100 times the before value for $Q/A$) and highly variable, providing a clue that this circuit model does not meaningfully describe these skin samples. As discussed further below, the dielectric constant is proportional to $(Q/A)^{1/\alpha}$. Thus, a 100-fold increase in $Q/A$ for $\alpha = 0.7$ (average of the three skin samples treated with DMSO

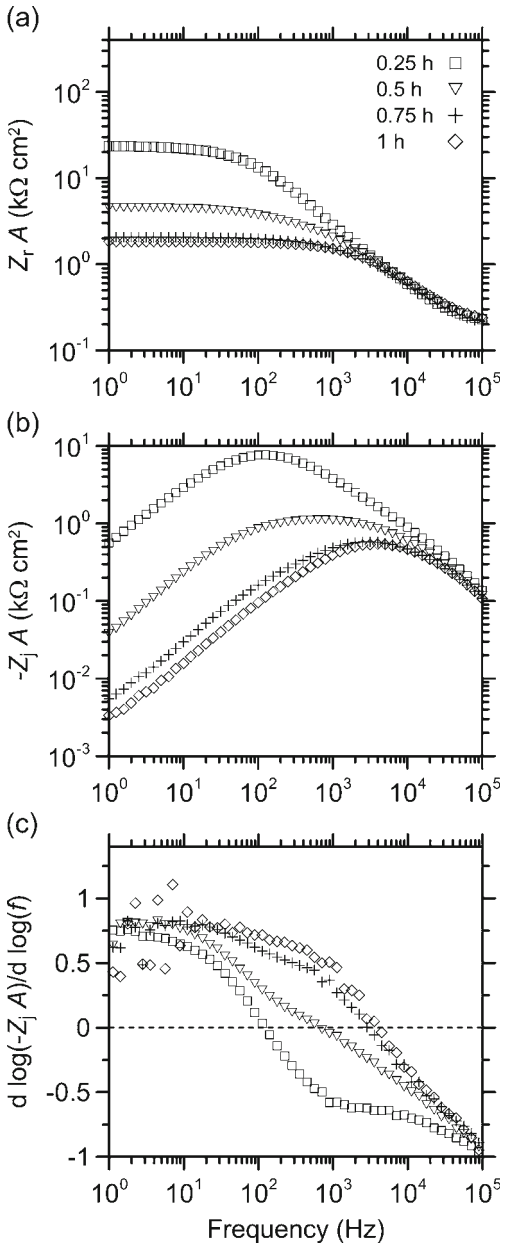


**Fig. 6** Impedance spectra plotted as a function of frequency for skin samples after treatment with DMSO for 0.25, 0.5, 0.75 and 1 h: (**a**) area normalized real part of the impedance, (**b**) area normalized imaginary part of the impedance, and (**c**) local slope of the log-log plot of the area normalized imaginary part of the impedance with frequency.

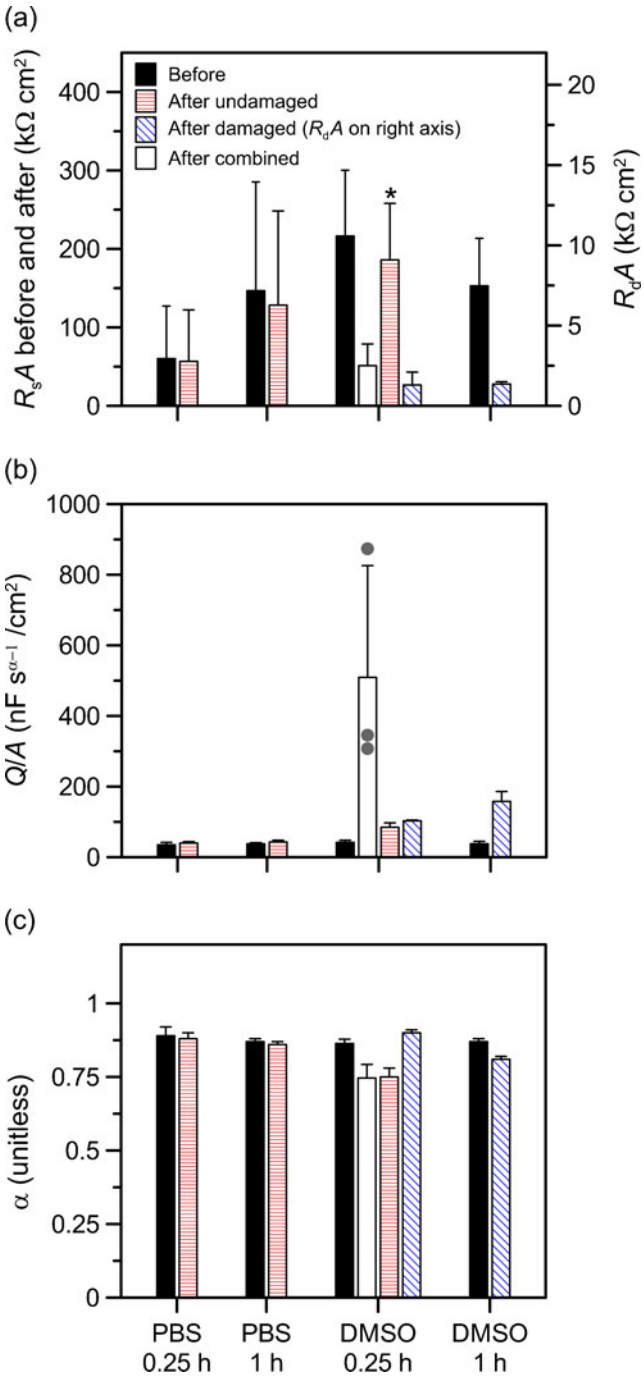


**Fig. 7** Parameters of the one or two R-CPE circuit models obtained by regression to impedance spectra before and after PBS (control) and DMSO treatments for 0.25 and 1 h (error bars designate one standard deviation for 3 replicates): (**a**) area normalized skin resistance, (**b**) area normalized CPE parameter $Q$, and (**c**) CPE parameter $\alpha$. Results are presented for the SC before treatment (Before), for the undamaged SC after PBS treatment or the undamaged SC layer of the 0.25 h DMSO treatment (After undamaged), for the damaged SC after 1 h DMSO treatment or the damaged SC layer after 0.25 h DMSO treatment (After damaged), and for the damaged and undamaged layers after the 0.25 h DMSO treatment regressed to the single R-CPE model circuit (After combined) with individual data points indicated as circles for $Q/A$. The parameters for the damaged and undamaged layers after 0.25 h DMSO treatment were calculated by assuming the resistance of the undamaged layer (designated with an asterisk) was 0.86 of the resistance before treatment, which was the average ratio for the PBS controls.

for 0.25 h) would correspond to an impossible 700-fold increase in the dielectric constant. These large values for $Q/A$ derived using the single R-CPE model arise because there was a significant decrease in $R_d A$ with no change in the characteristic frequency (see Eq. (2)). (The after-to-before ratio of the characteristic frequency calculated using the one R-CPE model was $1.07 \pm 0.13$; see Table S.I in the Supplementary Material.)

In Fig. 8 impedance data are compared for two samples before and after DMSO treatment to the fraction-damaged

model calculated using the regressed parameters. The results for both skin samples before treatment are shown in the left column. The results after treatment for 0.25 h (sample B) and 1 h (sample E) are presented in the middle and right columns, respectively. The results are presented in terms of the real ($\mathcal{Z}_r A$) and imaginary ($-\mathcal{Z}_j A$) components of the impedance plotted as functions of frequency in Figs. 8a and b, respectively, and as an impedance plane plot (Fig. 8c), which presents ($-\mathcal{Z}_j A$) plotted as a function of ($\mathcal{Z}_r A$).

The solid lines represent the total impedance calculated using the regressed models to the data. The dashed lines and the dot-dashed lines in the plots for the 0.25 h DMSO treatment represent the impedance calculated for the R-CPE elements corresponding to the undamaged and damaged SC layers, respectively: $(\widehat{\mathcal{Z}}_r + R_e)A$ for the damaged and undamaged layers in Fig. 8a, $(-\widehat{\mathcal{Z}}_j A)$ for the damaged and undamaged layers in Fig. 8b, and $(-\widehat{\mathcal{Z}}_j A)$ *versus* $(\widehat{\mathcal{Z}}_r + R_e)A$ for the damaged layer and $(-\widehat{\mathcal{Z}}_j A)$ *versus* $(\widehat{\mathcal{Z}}_r + R_e + R_d)A$ for the undamaged layer in Fig. 8c. The

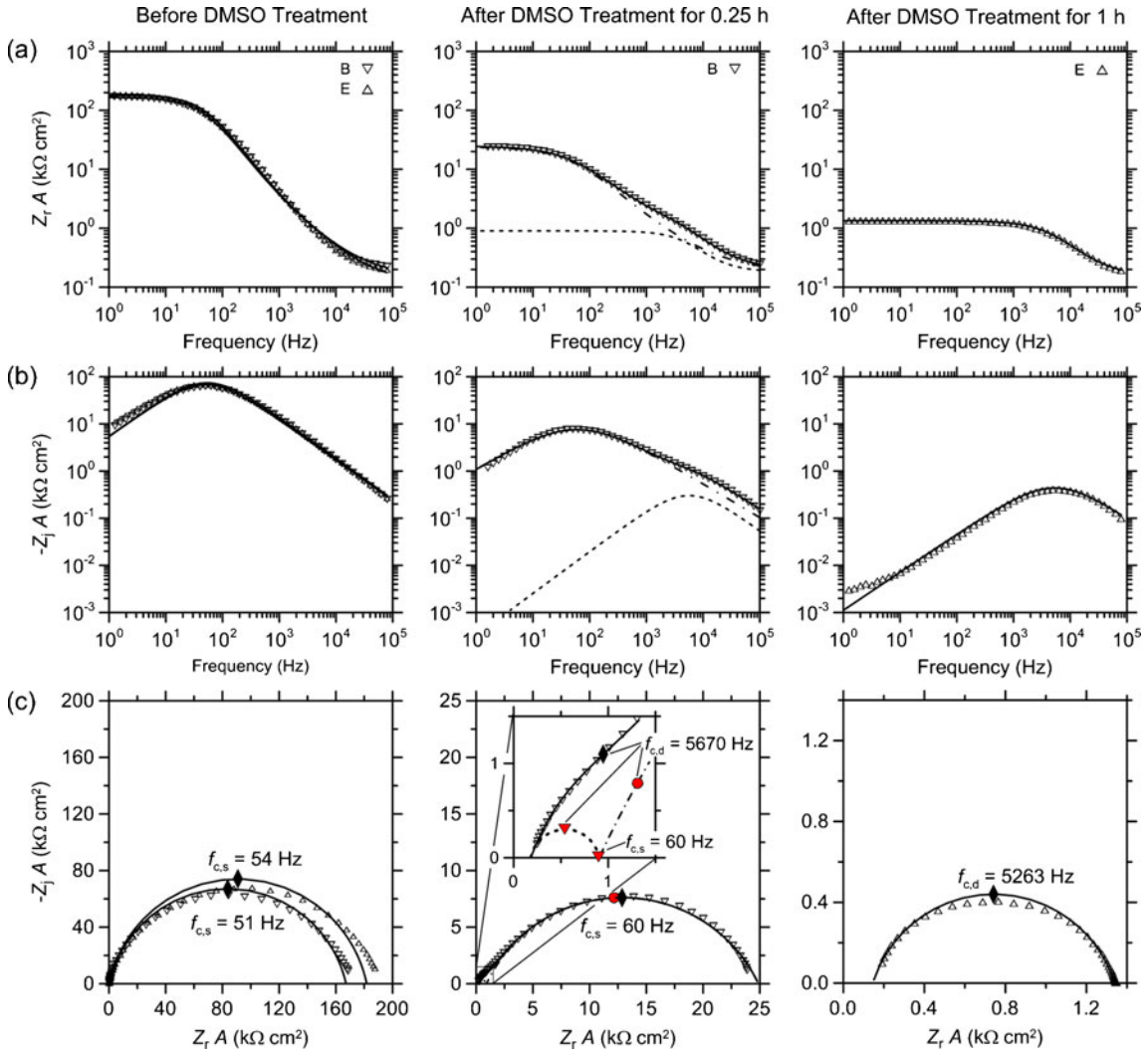


**Fig. 8** Example impedance spectra of skin before and after DMSO treatment for 0.25 h and 1 h compared to equivalent circuit models: (**a**) area normalized real part of the impedance *versus* frequency, (**b**) area normalized imaginary part of the impedance *versus* frequency, and (**c**) impedance plane (Nyquist) plot. The solid lines represent the total impedance derived by regression of the single R-CPE circuit model to data measured before DMSO and after DMSO treatment for 1 h, and regression of the fraction-damaged (two R-CPE circuit) model to the data measured after DMSO treatment for 0.25 h. The dashed lines and the dot-dashed lines respectively represent the impedance of the damaged and undamaged skin fractions after DMSO treatment for 0.25 h, specifically plotted as: (**a**) $(\widehat{\mathcal{Z}}_r + R_e)A$, (**b**) $-\widehat{\mathcal{Z}}_j A$, and (**c**) $-\widehat{\mathcal{Z}}_j A$ *versus* $(\widehat{\mathcal{Z}}_r + R_e)A$ for the damaged layer and $-\widehat{\mathcal{Z}}_j A$ *versus* $(\widehat{\mathcal{Z}}_r + R_e + R_d)A$ for the undamaged layer. The filled diamonds designate the model values at the characteristic frequency before and after DMSO treatment for 1 h. For skin treated with DMSO for 0.25 h, the characteristic frequencies of the undamaged and damaged layers (at 60 and 5,670 Hz, respectively) are designated for model values of the total impedance (*diamonds*), and also for the impedance of the undamaged (*circles*) and damaged (*triangles*) layers.

filled symbols in the three impedance plane plots (Fig. 8c) designate the theoretical values for $(-\mathcal{Z}_j A)$ and $(\mathcal{Z}_r A)$ values at the characteristic frequencies of the models. For skin treated with DMSO for 0.25 h, the characteristic frequencies of the undamaged and damaged layers (i.e., 60 and 5,670 Hz, respectively) are designated for the total impedance (diamonds) and also for the impedance of the undamaged (circles) and damaged (triangles) layers.

Before DMSO treatment, the impedance spectra of the two skin samples were nearly identical, with small differences that are primarily visible in the impedance plane plot (Fig. 8c). Although the maximum values of $\mathcal{Z}_r A$, determined at the lowest measured frequency, are noticeably different for the two samples in Fig. 8c, the characteristic frequencies are almost the same, indicating that the CPE parameters were slightly different for the two samples.

After DMSO treatment for 0.25 h, the impedance of the damaged layer, represented by the dashed lines, contributes little to the total impedance for frequencies below ~1,000 Hz. However, the shape and magnitude of the impedance response of the damaged layer (dashed lines) after 0.25 h DMSO treatment are similar to that of skin treated with DMSO for 1 h shown in the right column (note the change in scales in the three impedance plane plots).

The data for skin treated with DMSO for 1 h are in good agreement with the one R-CPE model except for $-\mathcal{Z}_j A$ measured at frequencies below about 5 Hz. A similar behavior has been observed in spectra from other samples that are not shown here. Data over the entire spectrum were shown to be consistent with the Kramers-Kronig relations using the measurement model method described by Agarwal *et al.* (32–35). Therefore, the deviation between model and data is most probably not an experimental artifact and a different model is required to capture the low frequency dispersion observed in these samples.

The d $\log(-\mathcal{Z}_j A)$/d $\log(f)$ spectra of samples B and E after DMSO treatment are shown in Fig. 9 with lines representing the fraction-damaged and one R-CPE models, respectively. The diamonds designate the theoretical value of the local slope at $f_{c,d}$ for the sample treated for 1 h (sample E) and at $f_{c,s}$ and $f_{c,d}$ for the sample treated for 0.25 h (sample B). When the data are presented this way, the similarity in the $f_{c,d}$ values for both treatment times is evident.

If the impedance response of the 0.25 h DMSO treated skin is consistent with the fraction-damaged model given by Eqs. (3) or (4), then the characteristic frequency estimated for the undamaged SC layer ($f_{c,s}$) should be similar to skin before DMSO treatment as well as to skin samples in the control experiments that were treated with PBS. Likewise, the characteristic frequency estimated for the damaged layer ($f_{c,d}$) should be similar to $f_{c,d}$ for skin treated with DMSO for 1 h. This is the case. The mean value of $f_{c,s}$ for samples A, B and C after 0.25 h DMSO treatment (45 ± 24 Hz) is statistically indistinguishable from the mean value of $f_{c,s}$ for the same three samples before 0.25 h DMSO treatment (41 ± 17 Hz). Also, the mean value of $f_{c,s}$ for samples A, B and C after 0.25 h DMSO treatment is statistically indistinguishable from the mean $f_{c,s}$ for all 12 samples before DMSO and PBS treatment (178 ± 244 Hz). Furthermore, the mean value of $f_{c,d}$ for samples A, B and C after 0.25 h DMSO treatment (4,150 ± 2,750 Hz) is statistically indistinguishable from the mean value of $f_{c,d}$ values samples D, E and F after 1 h DMSO treatment (5,640 ± 420 Hz). (Characteristic frequencies for individual skin samples and treatments are listed in Tables S.I and S.III of the Supplementary Material.)

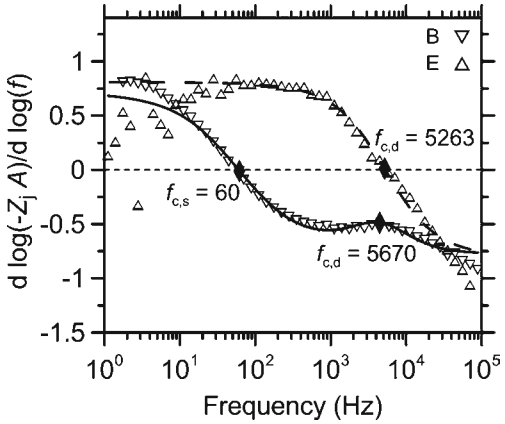


**Fig. 9** The first derivative of the logarithm of $(-\mathcal{Z}_j A)$ with respect to the logarithm of frequency as a function of the average frequency for skin samples that had been treated with DMSO for 0.25 and 1 h compared respectively to the fraction-damaged model of two R-CPE circuits in series (*solid lines*) and the one R-CPE circuit model (*dashed lines*)

In Fig. 10 the characteristic frequencies of the undamaged and damaged layers are compared graphically

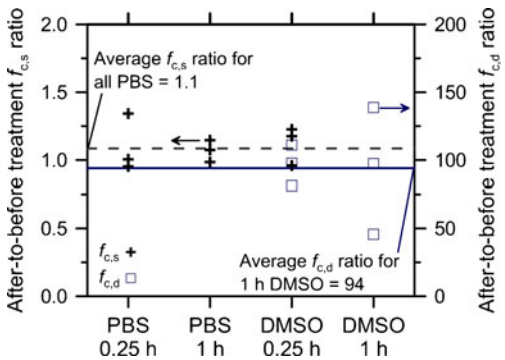


**Fig. 10** The after-to-before treatment ratio of the characteristic frequencies estimated for the undamaged ($f_{c,s}$) and damaged ($f_{c,d}$) layers of skin treated with DMSO for 0.25 h compared to skin treated with PBS and with DMSO for 1 h. The dashed line indicates the mean value of the ratio for all of the PBS control experiments ($f_{c,s}/f_{c,s\ before} = 1.1$), and the solid line represents the mean value of the ratio for skin treated with DMSO for 1 h DMSO experiments ($f_{c,d}/f_{c,s\ before} = 94$).

as the ratios of the characteristic frequencies after-to-before treatment with DMSO for 0.25 h (i.e., $f_{c,s}/f_{c,s\ \text{before}}$ and $f_{c,d}/f_{c,s\ \text{before}}$, respectively) to the after-to-before ratios from skin treated for 1 h with DMSO and for 0.25 h and 1 h with PBS. The dashed line, plotted on the left-hand axis at 1.1, represents the mean value of $f_{c,s}/f_{c,s\ \text{before}}$ for the six PBS control experiments. The solid line plotted on the right-hand axis at 94, designates the mean value of $f_{c,d}/f_{c,s\ \text{before}}$ from the three skin samples treated with DMSO for 1 h. Consistent with the assumption of the fraction-damaged model, the after-to-before ratios of the characteristic frequencies for the undamaged and damaged layers of skin treated with DMSO for 0.25 h are similar to the ratios observed after treatment with PBS at both treatment times and with DMSO for 1 h, respectively.

Values for $x_d/L$ for skin treated with DMSO for 0.25 h were estimated by requiring that the resistances of the two SC layers sum to give the total resistance observed experimentally expressed as

$$\widehat{R}_s + \widehat{R}_d = R_s\left(1 - x_d\Big/L\right) + R_d x_d\Big/L \tag{12}$$

which after rearrangement gives

$$x_d\Big/L = \frac{R_s - \left(\widehat{R}_s + \widehat{R}_d\right)}{R_s - R_d} \tag{13}$$

In addition, it was assumed that: (a) $R_d\,A$ is equal to the mean value of the resistance measured in skin treated with DMSO for 1 h (1.36 kΩ cm$^2$), and (b) $R_s\,A$ is equal to the resistance determined in the same piece of skin before treatment multiplied by 0.86, which was the average change in $R_s\,A$ observed in treatment with PBS for 0.25 and 1 h combined (see Fig. 7a). Calculated values for $x_d/L$ for each of the three samples treated with DMSO for 0.25 h (0.74 ± 0.076) were used to calculate the length-independent values of $Q/A$ for the damaged and undamaged layers, which are summarized in Fig. 7b (and detailed in Table S.IV in the Supplementary Material).

Regressed values for $\widehat{R}_s$ and $\widehat{R}_d$ were not available for skin samples exposed to DSMO for 0.5 and 0.75 h in the treatment-time study (data shown in Fig. 6) because the contribution of the undamaged layer was too small to reliably resolve meaningful estimates of the parameters in the two R-CPE circuit model. Therefore, values of $x_d\ /L$ for the four experiments in the pilot DMSO treatment-time study were estimated using the difference of $Z_r$ measured at low and high frequencies before DMSO treatment for $R_s$ and after DMSO treatment for $\widehat{R}_s + \widehat{R}_d$; results are listed in Table 1 along with those for skin samples treated with DMSO for 0.25 h. As noted in the discussion of Fig. 6, $x_d/L$ was essentially 1 for the sample treated with DMSO for 0.75 h.

If, as expected, the growth of the damaged layer is a diffusion process, then the plot of $x_d/L$ (for $x_d/L < 1$) *versus* the square-root of time forced through the origin should be linear (see Appendix for a more complete explanation). As shown in Fig. 11, this appears to be the case. The slope of the line in Fig. 11 is 1.5 h$^{-1/2}$, from which it can be estimated that $x_d/L$ should be equal to one for treatment times longer than about 0.5 h.

To estimate the lag time for the growth of the damaged layer requires an assumption about the smallest DMSO concentration relative to the maximum that causes an irreversible change in the electrical properties of the SC (see Appendix). For example, the lag time of the growth in the damaged layer thickness is almost 6 min if the concentration of DMSO in the damaged layer must be at least 50% of the maximum. For comparison, estimates for the lag time increase to about 25 min if the DMSO concentration needs to be at least 75% of the maximum, and decrease to 2 min if the concentration only needs to be 25% of the maximum. The observation that the time required to reach maximum effect is approximately 0.5 h is consistent with the requirement that DMSO concentration needs to be roughly 75% of the maximum concentration.

## Dielectric Constant

It has been proposed that chemical alteration of lipid layers in the SC would be reflected in changes to its effective dielectric constant (ε), which is related to the effective capacitance ($C_s$) by the following expression

**Table I** Estimates of the Area Normalized Total Skin Resistance Before and After DMSO Treatment and the Relative Thickness of the Damaged Layer ($x_d$/L) in the Treatment-Time Study Compared with the Study of DMSO Treatment for 0.25 h

| Treatment time h | Sample ID | Before DMSO $R_s\,A$ (kΩ cm$^2$) | After DMSO $(\widehat{R}_s + \widehat{R}_d)A$ (kΩ cm$^2$) | $x_d$/L |
|---|---|---|---|---|
| 0.25 | A | 313.3 | 78.5 | 0.75 |
| 0.25 | B | 167.0 | 24.7 | 0.86 |
| 0.25 | C | 169 | 45.5 | 0.74 |
| 0.25 | G | 114.0 | 23.4 | 0.80 |
| 0.50 | H | 185.7 | 4.34 | 0.98 |
| 0.75 | I | 340.7 | 1.87 | 1.00 |

Area normalized resistance values after DMSO treatment for 0.25 h (Samples A, B, and C) were determined by best-fit regression of the impedance spectrum to the two R-CPE model; area normalized resistance values in the treatment-time study were determined from the difference of $Z_r\,A$ measured at low and high frequencies before and after DMSO treatment

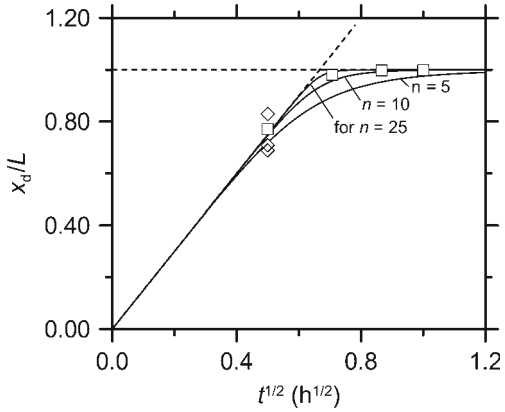


**Fig. 11** Calculated experimental values for the thickness of the damaged stratum corneum fraction ($x_d/L$) plotted as a function of the square-root of the DMSO treatment time for the 0.25 h DMSO experiments (*diamonds*) and the treatment-time study (*squares*). Solid lines represent the interpolation formula presented as Eq. (A6) in the Appendix with exponent $n$ as a parameter.

$$\varepsilon = \frac{\left(C_s/A\right)L}{\varepsilon_0} \tag{14}$$

where $L$ is the SC thickness and $\varepsilon_0$ is the permittivity of vacuum ($8.8542\times10^{-5}$ nF/cm). The problem then is to derive a value for $C_s$ from the R-CPE circuit parameters. Various formulas have been proposed. However, as discussed in the related paper describing impedance spectra measured before and after needle puncture (2), formulas that include $R_s$ in the calculation for $C_s$ generally produce physically unrealistic values for $\varepsilon$. Reasonable values for $\varepsilon$ are derived using the power-law formula proposed by Hirschorn *et al.* (36,37) to estimate the effective capacitance, designated as $C_{s,PL}$ (2)

$$C_{s,PL}/A = g^{1/\alpha_s}\left(Q_s/A\right)^{1/\alpha_s}(\delta\rho_\delta)^{(1-\alpha_s)/\alpha_s} \tag{15}$$

where $\rho_\delta$ is the resistivity at position $\delta$ perpendicular from the surface; this will be the resistivity of the innermost interface of the dominant resistive layer, which is the SC in the case of skin. The parameter $g$, defined as

$$g = 1 + 2.88(1-\alpha_s)^{2.375} \tag{16}$$

has a value near one for values of $\alpha_s$ that are typical for skin (i.e., between 0.8 and 0.9).

Although estimates of $\varepsilon$ from $C_{s,PL}$ require values for $\delta$ and $\rho_\delta$, the dependence is weak because $(\delta\rho_\delta)$ is raised to the power $(1-\alpha_s)/\alpha_s$, which is typically 0.25 or smaller. The minimum value for $\rho_\delta$ is the resistivity of the solution, which for PBS in our experiments was 55 Ω cm (2). If $\rho_\delta$ is 10× larger (i.e., 550 Ω cm), then the estimate for $\varepsilon$ increases by about only 1.6 (for $\alpha_s=0.8$).

Assuming $(\delta\ \rho_\delta)$ and the SC thickness $L$ are almost the same before and after DMSO treatment for 1 h, then the ratio of the $\varepsilon$ for the damaged to undamaged SC is

$$\frac{\varepsilon_d}{\varepsilon_s} = \frac{g^{1/\alpha_d}\left(Q_d/A\right)^{1/\alpha_d}}{g^{1/\alpha_s}\left(Q_s/A\right)^{1/\alpha_s}} \tag{17}$$

Using the average values for the three skin samples studied ($\alpha_s=0.87$, $\alpha_d=0.81$, $Q_s/A=38$ nF $s^{\alpha_s-1}/cm^2$, and $Q_d/A=158$ nF $s^{\alpha_s-1}/cm^2$; see Table S.II in the Supplementary Material), $\varepsilon$ after DMSO treatment is estimated to increase about 40%. The cause of this increase, if real, is unknown. However, it is consistent with damage or extraction that allows small amounts of lipids to be replaced with water, for which $\varepsilon$ is close to 80 compared with about 3 for oils.

## Chemical Flux

The steady-state flux of PCNB through skin measured before and after treatments with DMSO and PBS treatment for 0.25 h and 1 h are summarized in Fig. 12 (and reported in detail in Table S.V of the Supplementary Material). The change in PCNB flux after treatment is also listed. The flux increased after treatment for all samples except for one sample treated with PBS for 0.25 h and one sample treated with PBS for 1 h. The average change in flux after DMSO treatment for 1 h was insignificantly larger than the average change in flux after DMSO treatment for 0.25 h and PBS treatment for 0.25 h and 1 h (student t-test, $p<0.05$). Neither treatment time nor treatment type had a discernible effect on PCNB flux through skin. Thus, although the impedance of skin decreased significantly when treated with DMSO, and the change was larger after 1 h compared to 0.25 h, the flux of PCNB did not change significantly after DMSO treatment for either 0.25 h or 1 h compared to the PBS control experiments. This differed from the treatment-time study in which the ratio of the flux of 4-cyanophenol after to before DMSO treatment did increase with increasing treatment time from almost 2 at 0.25 h to about 4 at 1 h. However, because this pilot investigation examined only one sample at each treatment time, it is unknown if these differences would be significant if the experiment had been replicated.

In nearly all previous studies of DMSO, chemical permeation through skin was measured from solutions containing DMSO, sometimes in the donor solution containing the chemical, sometimes in the receptor solution that receives the chemical, and sometimes in both the donor and receptor (19–21,25). In the presence of DMSO concentrations larger than about 60% by volume in water, penetration increased for all chemicals including ionized and polar chemicals (e.g., picric acid (20) and water (22)) as well

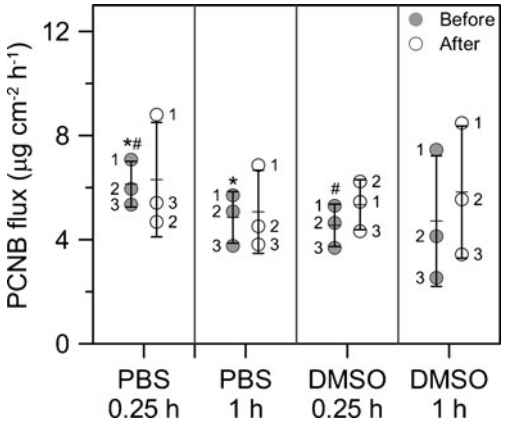


**Fig. 12** Comparison of the steady-state flux of PCNB measured before and after treatments with DMSO and PBS (control) for 0.25 and 1 h. Each sample in each treatment is identified by number and the error bars designate plus or minus one standard deviation from the mean. The fluxes measured before treatment, the fluxes measured after treatment, or the changes in fluxes from treatment were compared for a given treatment type (either PBS control or DMSO) and for a given treatment time (0.25 h and 1 h). For a given treatment type, only the fluxes measured before PBS treatments for 0.25 and 1 h (designated with *) were significantly different. For a given treatment time, only the fluxes measured before the 0.25 h treatment with DMSO were significantly different form the 0.25 h PBS control (designated with #). The variance for treatment times and treatment types were not statistically different from each other according to single-factor ANOVA.

as lipophilic chemicals (18,19,21,23,25,26). In these experiments, chemical permeation may have increased because DMSO damaged the SC or because large concentrations of DMSO within the SC may have increased the ability of chemicals to partition into the SC (29).

In this study chemical permeation was measured through SC that was damaged by DMSO but no longer contained DMSO. Therefore, the mechanism for enhanced penetration can only be irreversible damage. The significantly reduced resistance of the damaged SC indicates a large increase in the permeability of ions, which move in the polar pathway. This is entirely consistent with previous reports that tritiated water flux through skin from hairless mice increased about 90-fold after treatment with 90% DMSO for 0.5 h (22).

The PCNB flux results indicate that any effects of DMSO on the lipophilic pathway were too small to discern. This supports the hypothesis that irreversible SC damage arising from DMSO treatment for 1 h or less affects the lipophilic pathway negligibly. Given that 4-cyanophenol ($pK_a = 7.97$) is partially ionized in PBS buffered at pH of 7.4, an increase in the flux of its ionized species through the polar pathway might have been sufficient to give the measurable increase in total flux.

One study has reported an increased permeation of lipophilic compounds after DMSO exposure ended. In this investigation (19), DMSO exposure to isolated SC (prepared from neonatal rat skin) in both the donor and receptor chambers lasted long enough for permeation of an alcohol, either 1-propanol or 1-hexanol, to reach steady state; after this DMSO was rinsed from the SC and the steady-state permeation of the alcohol measured again. Alcohol permeation through the washed skin that had been exposed to DMSO concentrations of at least 80% was elevated compared with samples that had not been exposed to DMSO. Although the time of the DMSO exposure was unspecified, other information in the paper suggests that it may have been as long as 6 h. This would have been more than long enough for elution of components including lipids from the SC (23,25,27), which would have occurred to a much lesser extent in samples exposed to DMSO for 1 h or less as in the study presented here.

## CONCLUSIONS

Skin impedance measurements are sensitive to irreversible damage caused by exposure to 100% solutions of the polar solvent DMSO. Impedance measurements after DMSO treatment for various times between 0.25 h and 1 h were consistent with a circuit model in which it was assumed that DMSO progressively damaged a larger fraction of the skin thickness over time and that the undamaged fraction retained the electric properties of the skin before DMSO treatment. The impedance data were inconsistent with the theory that DMSO acts by increasing the contributions of low-resistance pathways through the SC. The skin appeared to be completely damaged after DMSO treatment times greater than about 0.5 h. If assumptions that the minimum local resistivity in the SC has changed minimally are correct, then the dielectric constant for fully damaged skin has increased by about 40%. This might be consistent with water replacing some fraction of the lipid. Despite changes in skin impedance, treating skin with DMSO for either 0.25 or 1 h did not change the flux of the moderately lipophilic molecule PCNB by a statistically significant amount. This indicates that exposure to DMSO for 1 h or less did not alter significantly the diffusion pathway for this lipophilic compound, although it did affect the pathway of ions and water and most probably other hydrophilic molecules.

This work demonstrates the manner in which, through comparison of experimental results to models derived from different hypotheses, impedance spectroscopy may be used to gain insight into a physical process. In the present work, impedance measurements allowed rejection of the hypothesis that DMSO damages skin by enhancing transport through channels. The impedance results were found to be consistent with the hypothesis that DMSO damages skin through a planar front. Models for impedance, however, are not unique and impedance spectroscopy should not be regarded as being a

stand-alone technique; thus, additional observations are needed. The additional analysis in terms of characteristic frequencies (Fig. 10) that showed two distinct layers, the slight increase after DMSO treatment found in dielectric constants obtained from regressed parameters, and the consistency of the damage front with diffusion (Fig. 11) provided additional support for the hypothesis that DMSO damage progresses through the skin as a distinct layer controlled by diffusion processes.

## ACKNOWLEDGMENTS AND DISCLOSURES

The authors acknowledge support from the National Institute of Occupational Safety and Health (application number 1-R01-OH007493).

## APPENDIX

Expressions for the real and imaginary components of the R-CPE circuit shown Fig. 1a

$$\mathcal{Z}_r = R_e + R_s\left[\frac{1 + Q_s R_s (2\pi f)^{\alpha_s}\cos\left(\alpha_s\pi/2\right)}{1 + R_s^2 Q_s^2 (2\pi f)^{2\alpha_s} + 2Q_s R_s (2\pi f)^{\alpha_s}\cos\left(\alpha_s\pi/2\right)}\right] \tag{A1}$$

and

$$\mathcal{Z}_j = \frac{-Q_s R_s^2 (2\pi f)^{\alpha_s}\sin\left(\alpha_s\pi/2\right)}{1 + R_s^2 Q_s^2 (2\pi f)^{2\alpha_s} + 2Q_s R_s (2\pi f)^{\alpha_s}\cos\left(\alpha_s\pi/2\right)} \tag{A2}$$

respectively, we used in calculations of the theoretical results.

Growth of the damaged skin layer appeared to be proportional to the square-root of time as expected for a diffusion based process as described here. The concentration of a chemical ($c$) within an initially chemical free membrane at time ($t$) soon after it is exposed to a chemical solution at constant concentration is expressed as

$$\frac{c}{c_o} = 1 - \mathrm{erf}\left(\frac{x/L}{2\sqrt{Dt/L^2}}\right) \tag{A3}$$

where $c_o$ is the concentration of chemical in the membrane at the surface in contact with the solution, $x$ is the position in the membrane from the surface in contact with the solution, $L$ is the membrane thickness, and $D$ is the diffusion coefficient of the chemical in the membrane (38). The growth in the thickness of the damaged layer ($x_d$), which is the position within the membrane where $c$ is equal to the minimum DMSO concentration required to alter the measured membrane properties ($c_d$), can be written by a rearrangement of Eq. (A3) as

$$x_d/L = 2\sqrt{Dt/L^2}\,\mathrm{erf}^{-1}\left(1 - c_d/c_o\right) \tag{A4}$$

It follows that the lag time for the growth in the damaged layer thickness ($t_{lag,d}$) can be expressed as

$$t_{lag,d} = \frac{L^2}{6D} = \frac{1}{24\left[\mathrm{erf}^{-1}\left(1 - c_d/c_o\right)\right]^2\left(\frac{x_d/L}{\sqrt{t}}\right)^2} \tag{A5}$$

Given $c_d/c_o$, estimates for $t_{lag,d}$ can be calculated by substituting the slope of a plot of $x_d/L$ versus the square-root of time for $(x_d/L)/\sqrt{t}$ in Eq. (A5).

An interpolation formula was developed to show the correspondence between the short-time behavior in which the growth of the DMSO-damaged layer increased with the square root of time and the long-time behavior in which the skin was fully damaged. The formula is given as

$$\frac{x_d}{L} = a\sqrt{t}\Big/\left(\left(a\sqrt{t}\right)^n + 1\right)^{1/n} \tag{A6}$$

where $n$ is an empirically determined constant and

$$a = 2\sqrt{D/L^2}\,\mathrm{erf}^{-1}\left(1 - c_d/c_o\right) \tag{A7}$$

The value of $n$ was found to be large ($\geq 25$) indicating that the transition from short-time to long-time behaviors was sharp (see Fig. 11). Thus, the slope ($a = 1.5\ \mathrm{h}^{-1/2}$) obtained from the origin and the data at 0.25 h provides an accurate assessment of the rate at which DMSO damaged the skin.

## REFERENCES

1. Orazem ME, Tribollet B. Electrochemical impedance spectroscopy. Hoboken: Wiley-Interscience; 2008.
2. White EA, Orazem ME, Bunge AL. Characterization of damaged skin by impedance spectroscopy: Mechanical damage. Pharm Res. 2013. doi:10.1007/s11095-013-1052-1
3. Leveque JL, Derigal J. Impedance methods for studying skin moisturization. J Soc Cosmet Chem. 1983;34(8):419–28.
4. Tagami H, Ohi M, Iwatsuki K, Kanamaru Y, Yamada M, Ichijo B. Evaluation of the skin surface hydration in vivo by electrical measurement. J Investig Dermatol. 1980;75(6):500–7.
5. Curdy C, Naik A, Kalia YN, Alberti I, Guy RH. Non-invasive assessment of the effect of formulation excipients on stratum corneum barrier function in vivo. Int J Pharm. 2004;271(1–2):251–6.
6. Clar EJ, Cambra M, Sturelle CG. Study of skin horny layer hydration and restoration by impedance measurement. Cosmet Toiletries. 1982;94:33–40.

7. Brogden NK, Milewski M, Ghosh P, Hardi L, Crofford LJ, Stinchcomb AL. Diclofenac delays micropore closure following microneedle treatment in human subjects. J Control Release. 2012;163(2):220–9.
8. Burnette RR, Bagniefski TM. Influence of constant current iontophoresis on the impedance and passive Na+ permeability of excised nude mouse skin. J Pharm Sci. 1988;77(6):492–7.
9. Curdy C, Kalia YN, Guy RH. Non-invasive assessment of the effects of iontophoresis on human skin in-vivo. J Pharm Pharmacol. 2001;53(6):769–77.
10. Curdy C, Kalia YN, Guy RH. Post-iontophoresis recovery of human skin impedance in vivo. Eur J Pharm Biopharm. 2002;53(1):15–21.
11. Kalia YN, Nonato LB, Guy RH. The effect of iontophoresis on skin barrier integrity: non-invasive evaluation by impedance spectroscopy and transepidermal water loss. Pharm Res. 1996;13(6):957–60.
12. Kumar MG, Lin SS. Transdermal iontophoresis: impact on skin integrity as evaluated by various methods. Crit Rev Ther Drug Carrier Syst. 2008;25(4):381–401.
13. Kim HS, Oh SY. Effect of polyoxyethylene alkyl esters on permeation enhancement and impedance of skin. Biol Ther. 2011;19(1):109–17.
14. Oh SY, Guy RH. The effect of oleic acid and propylene glycol on the electrical properties of skin. J Korean Pharm Sci. 1994;24(4):281–7.
15. Oh SY, Guy RH. Effect of enhancers on the electrical properties of skin: the effect of azone and ethanol. J Korean Pharm Sci. 1994;24(3):S41–7.
16. Oh SY, Leung L, Bommannan D, Guy RH, Potts RO. Effect of current, ionic strength and temperature on the electrical properties of skin. J Control Release. 1993;27(2):115–25.
17. Foley D, Corish J, Corrigan OI. The use of complex impedance to examine the effect of passive and iontophoretic transdermal drug transport through excised human epidermal tissue. Proc Int Symp Control Release Bioact Mater. 1990;17:427–8.
18. Klamerus K, Lee G. Effects of some hydrophilic permeation enhancers on the absorption of bepridil through excised human skin. Drug Dev Ind Pharm. 1992;18(13):1411–22.
19. Al-Saidan SM, Selkirk AB, Winfield AJ. Effect of dimethylsulfoxide concentration on the permeability of neonatal rat stratum corneum to alkanols. J Invest Dermatol. 1987;89(4):426–9.
20. Elfbaum SG, Laden K. The effect of dimethyl sulfoxide on percutaneous absorption: a mechanistic study, part I. J Soc Cosmet Chem. 1968;19:119–27.
21. Chandrasekaran SK, Campbell PS, Michaels AS. Effect of dimethyl sulfoxide on drug permeation through human skin. AIChE J. 1977;23(6):810–6.
22. Sweeney TM. The effect of dimethyl sulfoxide on the epidermal water barrier. J Invest Dermatol. 1966;46(3):300–2.
23. Kurihara-Bergstrom T, Flynn GL, Higuchi WI. Physicochemical study of percutaneous absorption enhancement by dimethyl sulfoxide: kinetic and thermodynamic determinants of dimethyl sulfoxide mediated mass transfer of alkanols. J Pharm Sci. 1986;75(5):479–86.
24. Allenby AC, Fletcher J, Schock C, Tees TFS. The effect of heat, pH and organic solvents on the electrical impedance and permeability of excised human skin. Br J Dermatol. 1969;81(4):31–9.
25. Allenby AC, Creasey NH, Edgington JAG, Fletcher JA, Schock C. Mechanism of action of accelerants on skin penetration. Br J Dermatol. 1969;81(Supplement 4):47–55.
26. Kurihara-Bergstrom T, Flynn GL, Higuchi WI. Physicochemical study of percutaneous absorption enhancement by dimethyl sulfoxide: Dimethyl sulfoxide mediation of vidarabine (ara-A) permeation of hairless mouse skin. J Invest Dermatol. 1987;89(3):274–80.
27. Embery G, Dugard PH. The isolation of dimethyl sulfoxide soluble components from human epidermal preparations: A possible mechanism of action of dimethyl sulfoxide in effecting percutaneous migration phenomena. J Invest Dermatol. 1971;57(5):308–11.
28. Anigbogu ANC, Williams AC, Barry BW, Edwards HGM. Fourier transform raman spectroscopy of interactions between the penetration enhancer dimethyl sulfoxide and human stratum corneum. Int J Pharm. 1995;125(2):265–82.
29. Barry BW. Mode of action of penetration enhancers in human skin. J Control Release. 1987;6:85–97.
30. Greve TM, Andersen KB, Nielsen OF. Penetration mechanism of dimethyl sulfoxide in human and pig ear skin: an ATR-FTIR and near-FT Raman spectroscopic in vivo and in vitro study. Spectroscopy. 2008;22(5):405–17.
31. Caspers PJ, Williams AC, Carter EA, Edwards HGM, Barry BW, Bruining HA, *et al*. Monitoring the penetration enhancer dimethyl sulfoxide in human stratum corneum in vivo by confocal Raman spectroscopy. Pharm Res. 2002;19(10):1577–80.
32. Agarwal P, Orazem ME, Garcia-Rubio LH. Measurement models for electrochemical impedance spectroscopy I. Demonstration of applicability. J Electrochem Soc. 1992;139:1917–26.
33. Agarwal P, Crisalle O, Orazem ME, Garcia-Rubio L. Application of measurement models to impedance spectroscopy, II. Determination of the stochastic contribution to the error structure. J Electrochem Soc. 1995;142(12):4149–58.
34. Agarwal P, Orazem ME, Garcia-Rubio L. Application of measurement models to impedance spectroscopy, III. Evaluation of consistency with Kramers-Kronig relations. J Electrochem Soc. 1995;142(12):4159–68.
35. Agarwal P, Orazem ME, Garcia-Rubio LH. The influence of error structure on interpretation of impedance spectra. Electrochim Acta. 1996;41(7/8):1017–22.
36. Hirschorn B, Orazem ME, Tribollet B, Vivier V, Frateur I, Musiani M. Constant-phase-element behavior caused by resistivity distributions in films I. Theory. J Electrochem Soc. 2010;157(12):C452–7.
37. Hirschorn B, Orazem ME, Tribollet B, Vivier V, Frateur I, Musiani M. Determination of effective capacitance and film thickness from constant-phase-element parameters. Electrochim Acta. 2010;55(21):6218–27.
38. Crank J. The mathematics of diffusion. 2nd ed. Oxford: Oxford Science Publication; 1975.